The Influence of Wind on the Water Age in the Tidal Rappahannock River

Wenping Gong, Jian Shen, Bo Hong

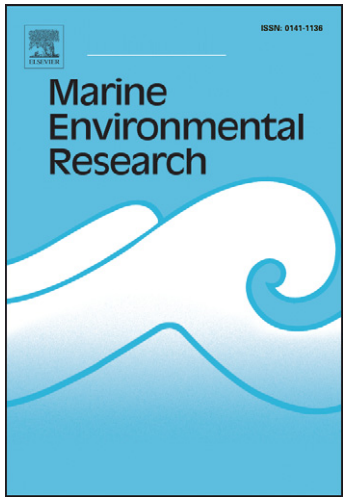

The Influence of Wind on the Water Age in the Tidal Rappahannock River

Wenping Gong, Jian Shen, Bo Hong

PII: S0141-1136(09)00071-3
DOI: 10.1016/j.marenvres.2009.06.008
Reference: MERE 3348

To appear in: *Marine Environmental Research*

Received Date: 28 September 2008
Revised Date: 26 May 2009
Accepted Date: 4 June 2009

Please cite this article as: Gong, W., Shen, J., Hong, B., The Influence of Wind on the Water Age in the Tidal Rappahannock River, *Marine Environmental Research* (2009), doi: 10.1016/j.marenvres.2009.06.008

The Influence of Wind on the Water Age in the Tidal Rappahannock River

Wenping Gong[a] Jian Shen[b*] Bo Hong[b]

[a]School of Marine Science, Sun Yat-Sen University, 135 Xingangxi Rd., Guangzhou 510275, China

[b]Virginia Institute of Marine Science, The College of William and Mary, Gloucester Point, VA., USA

Submitted to

Marine Environmental Research

*Corresponding Author:

Jian Shen

Virginia Institute of Marine Science

The College of William and Mary

1208 Greate Road

Gloucester Point, VA., USA

23062

Email: shen@vims.edu

Tel: 01-804-684-7359

The Influence of Wind on the Water Age in the Tidal Rappahannock River

Wenping Gong[a] Jian Shen[b*] Bo Hong[b]

[a]School of Marine Science, Sun Yat-Sen University, 135 Xingangxi Rd., Guangzhou 510275, China

[b]Virginia Institute of Marine Science, The School of Marine Science, The College of William and Mary, Gloucester Point, VA., USA

Abstract

Wind plays an important role in regulating mixing/stratification, estuarine circulation, and transport timescale in estuaries. A three-dimensional model was used to investigate the effect of wind on transport time by using the concept of water age (WA) in the tidal Rappahannock River, a western tributary of the Chesapeake Bay, USA. The model was calibrated for water level, current, and salinity. A series of experiments regarding the effects of wind on WA was conducted under various dynamic conditions. The effect of wind on transport timescale depends strongly on the competition between the wind and buoyancy forcings, and on the pre-status of the circulation. A down-estuary wind generally decreases WA along the estuary. An up-estuary wind increases WA substantially because it changes the vertical mixing and estuarine circulation more significantly. When the buoyancy forcing increases, the up-estuary wind effect decreases whereas the down-estuary wind effect increases. A 2-day period wind pulse with a maximum speed of 15 $m \cdot s^{-1}$ can alter WA for 3 days; but the wind influence on WA lasts up to 40 days in the simulation. Both local and non-local wind forcings alter WA

distribution. The local wind enhances vertical mixing and changes the gravitational circulation in the downstream portion of the estuary whereas it enhances transport in the freshwater portion of the estuary. Consequently, the local wind has a significant impact on WA distribution. In contrast, the non-local wind does not change the gravitational circulation significantly by imposing setup (setdown) of water level at the open boundary, resulting in a lesser impact on WA distribution.

Key words: Wind; water age; estuarine circulation; stratification; EFDC; Rappahannock River

1. Introduction

The amount of nutrients discharged into an estuary and the transport time required for these nutrients to be exported to the ocean, along with other biogeochemical processes, play important roles in the eutrophication processes of an estuary (Nixon, et al, 1996, Boynton et al., 1995). To quantify the transport timescale in lagoons, estuaries and oceans, the age concept of a water parcel has been introduced and utilized (e.g., Zimmerman, 1976; Takeoka, 1984; Deleersnijder et al., 2001; Beckers et al., 2001; Delhez and Deleersnijder, 2002; Shen and Haas, 2004; Shen and Lin, 2006; Shen and Wang, 2007). Following Delhez et al. (1999), the water age (WA) is defined in this study as the time elapsed since a dissolved substance is discharged into the estuary, and WA at any location is representative of the timescale for the dissolved substance to be transported from its source to that location. Delhez et al. (1999) introduced the water age

theory based on the advection-diffusion of a tracer and provided a general methodology to compute the age using an Eulerian-frame modeling approach. Delhez and Delleersnijder (2002) simulated the age of technetium-99 released from the Cap de La Hague nuclear fuel reprocessing plant in the English Channel successfully by using a 3-D model. The studies of WA in the tidal York River and James River indicate that WA depends highly on river discharge (Shen and Haas, 2004), and the transport timescale and vertical distribution relies on the strength of the gravitational circulation (Shen and Lin, 2006)

The characteristics of the transport processes for dissolved substances depend primarily on the low frequency and mean motions of the water in an estuary (McCarthy, 1993). For a given estuary, the variation of the low-frequency residual flow relies on the interactions of the density field, river flow, wind, and the nonlinear rectification of the periodic tides. The impact of river flow and tidal mixing on estuarine circulation evolves in different stages and depends on the competition between the buoyancy input and tidal amplitude (Park and Kuo, 1996; MacCready, 1999). Many researches have demonstrated that wind plays a dominant role in affecting stratification and non-tidal circulation in estuaries (Geyer, 1997; Sanay, 2003; North et al., 2004; Scully et al., 2005, Li et al., 2007). Scully et al. (2005) demonstrated that the influence of wind on stratification is the competition between wind straining and wind mixing. A down-estuary wind increases stratification, decreases the vertical eddy viscosity and enhances gravitational circulation. An opposite situation occurs for an up-estuary wind. Under less stratified conditions, the wind is more effective in creating mixing while wind straining can dominate over wind

stirring under more stratified situations. These results suggest that the effect of wind depends on the pre-status of mixing in the water column.

Besides investigating the vertical and longitudinal structure of estuarine circulation, recent studies also focused on their transverse structure (e.g., Guo and Valle-Levinson, 2008). For a cross-section with a channel and side shoals in the estuaries, the net flow is in the direction of the density gradient or of the local winds over the two shallow sides whereas a reversed net flow develops at the channel (Wong, 1994; Friedrichs and Hamrick, 1996). For a down-estuary wind, the wind-driven and buoyancy-induced flows are additive, and the lateral structure of the estuarine flows is enhanced (Wong, 1994; Friedrichs and Hamrick, 1996). With an up-estuary wind forcing, the effect of wind on the estuarine circulation is controlled by the relative importance of the wind and buoyancy forcings, which can be represented by a Wedderburn number (Geyer, 1997; Sanay, 2003):

$$W_e = \frac{l\tau_s}{g\bar{h}^2\Delta\rho} \tag{1}$$

where τ_s is the wind stress, l is the salt intrusion length, g is the gravity acceleration of gravity, $\bar{h}$ is the mean water depth and $\Delta\rho / l$ is the horizontal density gradient. A strong up-estuary wind will induce a transverse structure of flow (with upstream flows along the side shoals and downstream flows at the channel) while a weak up-estuary wind can not alter the gravitational circulation driven by the buoyancy force.

The study concerning the effect of wind on WA is limited. Shen and Wang (2007) examined the influence of wind on WA and transport timescale in the Chesapeake Bay. It was found that the influences of wind on the spatial and temporal distribution of WA

depend on both the magnitude and direction of the wind. The up-estuary wind increases the transport time and the down-estuary wind decreases the transport time in the model simulations. Gustafsson and Bendtsen (2007) studied the effect of wind on WA in a shallow estuary in Denmark. The results indicated that surface salinity and WA decreased due to the reduced vertical mixing and stratification increased if the wind was turned off in the model, and the fresh water runoff was effectively confined in the surface layer. Their results are relevant for shallow fjords where wind is the major vertical mixing agent. Conversely, the variations of water level, current, and mass transport in a tributary are highly affected by the non-local wind forcing (Elliott, 1976; Wang and Elliot, 1978; Elliott, 1978; Sanford and Boicourt, 1990). It is reasonable to speculate that the non-local wind effect can additionally impact the transport timescale in a tributary. The above results indicate that the influence of wind on WA is complex and warrants further investigation.

A three-dimensional Environmental Fluid Dynamics Code (EFDC) developed by Hamrick (1992) was used in this study to investigate the effect of wind on WA in the Rappahannock River. The model was calibrated with the available water elevation, current and salinity data. A series of numerical simulations were conducted to investigate the effect of wind on transport timescales and their corresponding mechanisms under various dynamic conditions. The interactions among the density field, river flow, and wind, and their influences on WA were examined. The effects of local and non-local winds on WA were explored.

2. Study site

The Rappahannock River is one of the major tributaries of the Chesapeake Bay (Fig. 1). The cross-sectional areas of the estuary increase exponentially as the shore widens from about 0.2 km at the headwater to 5 km at the mouth and the channel deepens from 5 to 24 m. The drainage area above the fall line is 4132 km^2. The stream flow (based on the data from 2000 to 2007) at the USGS gauging station near Fredericksburg, Virginia (ID 01668000), shows that the low flow discharge (10^{th} percentile) is 13.56 m^3s^{-1}, the mean flow rate (50^{th} percentile) is 37.66 m^3s^{-1}, and the high flow (95^{th} percentile) is 182.36 m^3s^{-1}. The principal tidal component is the lunar semi-diurnal tide with a period of 12.42 hours. The mean tidal range is 37 cm near the mouth and the tidal wave takes about 9 hours to propagate from the river mouth to the fall line (Park, 1993). The lower portion of the tidal Rappahannock River is a partially mixed estuary. The salt water intrusion is generally located around 120 km from the mouth during low-flow and around 70 km during high-flow. The Rappahannock River is characterized by persistent hypoxic conditions in the bottom water from the mouth to 50 km upstream during the summer; this is partly attributed to the weak gravitational circulation of the estuary (Kuo and Nelson, 1987).

The wind data of 2006 at the NOAA station of Lewisetta (ID 8635750) show that the most frequent winds are southwesterly and northwesterly with a mean wind velocity of 4.2 and 5.0 $m{\cdot}s^{-1}$, respectively. The wind is relatively weak during the summer when the southwesterly wind prevails. The northeasterly and northwesterly winds usually dominate the winter season. As wind plays an important role for the hydrodynamics and water

quality in the Rappahannock River, it is an ideal place for studying the wind effect on the transport timescale.

3. Methodology

3.1. Numerical model

The EFDC model was used to simulate water level, current, salinity, tracer concentration, and WA in this study. The model solves the three-dimensional continuity and free surface equations of motion (Hamrick, 1992a; Hamrick and Wu, 1997). The Mellor and Yamada level 2.5 turbulence closure scheme is implemented in the model (Mellor and Yamada, 1982; Galperin et al., 1988). The model uses stretched (or sigma) vertical coordinates and curvilinear, orthogonal horizontal coordinates. It simulates density and topographically-induced circulation, tidal and wind-driven flows, and spatial and temporal distributions of salinity, temperature, and conservative/non-conservative tracers. The model has been successfully applied to a wide range of environmental studies (e.g. Shen and Haas, 2004; Shen and Lin, 2006; Gong et al., 2007; Xia et al., 2007).

Rectangular Cartesian grids were used in most portions of the Rappahannock River with a cell size of 200 m in both x and y directions. Because the upper portion of the estuary becomes narrow and meandering, curvilinear grids were used to better fit the shoreline in this upstream portion. The grid resolution ranged from 200 m to 1400 m. Six layers were used in the vertical direction. The open boundary was extended a short distance out of the estuary mouth to avoid any influence of the boundary condition on the circulation near the mouth. The model domain is shown in Fig.1. The bathymetry data

from the NGDC (National Geophysical Data Center) were interpolated into the model grids (http://www.ngdc.noaa.gov/mgg/coastal/coastal.html).

3.2 Age calculation

Several methods have been introduced for computing WA (Bolin and Rodhe, 1972; Zimmerman, 1976; Takeoka, 1984). Delhez et al (1999) provided a general method using numerical models to compute spatially varying WA distributions in a real estuarine environment. WA can be computed based on a tracer and age concentrations. Assuming that there is only one tracer discharged into the system without other sources and sinks, the transport equations for calculating the tracer and age concentrations can be written as (Deleersnijder et al., 2001):

$$\frac{\partial c(t,\vec{x})}{\partial t} + \nabla(\vec{u}c(t,\vec{x}) - K\nabla c(t,\vec{x})) = 0 \quad (2)$$

$$\frac{\partial \alpha(t,\vec{x})}{\partial t} + \nabla(\vec{u}\alpha(t,\vec{x}) - K\nabla \alpha(t,\vec{x})) = c(t,\vec{x}) \quad (3)$$

where c is the tracer concentration, α is the age concentration, $\vec{u}$ is the velocity field in space and time domains, K is the diffusivity tensor, t is time and $\vec{x}$ is coordinate. The WA "a"can be calculated as:

$$a(t,\vec{x}) = \frac{\alpha(t,\vec{x})}{c(t,\vec{x})} \quad (4)$$

The vertically averaged WA can be computed by averaging WA at each layer.

3.3 Model setup

A radiation boundary condition was used for the water level at the open boundary to allow the outgoing wave to propagate out of the model domain freely. For the model calibration, the observed water level data at the NOAA Windmill Point gauge station (ID 8636580) were used as an incoming wave. The salinity data from the LE3.6 station, measured monthly by the Chesapeake Bay Program (http://www.chesapeakebay.net), were linearly interpolated both spatially and temporally during the simulation period and used as the incoming salinity at the open boundary. The salinity at ebb tide at the open boundary was calculated using upwind concentrations immediately inside the open boundary. When the flow at the open boundary changed from outflow to inflow, the model provided a linear interpolation based on the last outflowing salinity and the specified incoming salinity within a specified time interval (Yang and Hamrick, 2005). At the estuary headwater, daily freshwater discharge measured at the USGS gauge station near Fredericksburg, Virginia was utilized. The wind data at the NOAA station of Lewisetta (ID 8635750) were applied to force the model at the water surface.

The model's initial condition was obtained by running the model iteratively until the modeled salinity distribution reached the quasi-equilibrium state. The open boundary condition of WA was treated the same as the salinity except that the incoming tracer and age concentrations were set to zero. The tracer with a concentration of 1 (arbitrary units) was continuously released at the headwater of the River.

Five sets of numerical experiments (Table 1) were conducted for investigating the effects of wind on WA, which are grouped as: (1) real-time down-estuary and up-estuary wind effects (E01-E03); (2) local and non-local wind effects (E11 and E12); (3) wind pulse effect (E21 and E22); (4) constant wind effect (E31-E33); and (5) river discharge

and wind interaction (E41-E43). As the alignment of the Rappahannock River is in a northwest direction, winds from the northwest and southeast directions were used for the down-estuary and up-estuary winds, respectively.

All the setup details of the experiments are described in Table 1. Experiment E00 is the simulation forced by real observations and is referred to as the Real Case hereafter. For experiment E02-03, the real-time wind vectors were projected on the northwest-southeast axis and only downstream or upstream components were used as wind forcings for E02 or E03, respectively. For experiments E11-E12, the non-local wind effect was examined by conducting E11 using the same observed wind forcing, river discharge, and salinity at the boundary as those in E00, except that the water level at the open boundary was replaced by astronomical tides. The difference between E11 and E00 represents the non-local wind effect. The local wind effect was studied by specifying the observed water level at the open boundary without wind forcing in the estuary (E12). The difference between E12 and E00 denotes the local wind effect. For the wind pulse study (E21 and E22), a half sinusoidal function for the wind velocity was specified as wind forcing. Wind started on Day 200 and reached a maximum magnitude of 15 $m \cdot s^{-1}$ on Day 201, and waned for another day. After Day 202, the wind was stopped. This wind pulse represents a typical strong wind event in the Chesapeake Bay region. For E31-E33, down- and up-estuary winds were set as 5 $m \cdot s^{-1}$ from the northwest and southeast directions, to represent the mean wind conditions in the Rappahannock River. For E41-E43, the 95th percentile high flow was utilized as the upstream boundary condition.

4. Model calibration

4.1. Water elevation

The water elevation was calibrated by adjusting the bottom roughness height (z_0) to make the modeled water elevations along the estuary agree with the predicted mean tide characteristics in the tidal table (National Ocean Survey, 1989). A mean freshwater inflow was specified at the upstream boundary as it does not affect the mean tidal range along the estuary (Park, 1993). A sinusoidal (M_2) tide with a range of 0.37 cm was specified at the open boundary. The model result is shown in Fig. 2. It can be seen that the modeled mean tidal range compares favorably with the observations, which indicates that the characteristics of the tidal propagation from the mouth to the headwater is well represented by the model (Park, 1993). As the tide propagates upstream (with the decreasing of cross-section area), the tidal range increases from the mouth to 55 km upstream. With the superposition of a reflected wave, a nodal point is located approximately 100 km from the mouth. Beyond the nodal point, the tidal range continues to increase towards the headwater.

4.2. Current

For the current calibration, the available measurements in the summer of 1987 (lasted approximately one month from 8/4 to 9/3) was collected. The detailed description of the field observation can be found in Kuo and Moustafa (1989). The stations for current measurements are shown in Fig. 1. The open boundary conditions of the model for water level and salinity was set the same as Park (1993). The wind forcing data at Gloucester Point (Fig.1) during the simulation period was applied to the model. The river discharge data at the USGS gauge station near Fredericksburg, Virginia was utilized for the

upstream boundary condition. The initial salinity field was interpolated from the data measured on 8/4/1987. A comparison between the model results and observations are shown in Fig. 3. The modeled velocities almost agree with the observations. The Mean Error, Mean Absolute Error, and Mean Absolute Relative Error between the model results and observations were as follows: 0.04 ms^{-1}, 0.08 ms^{-1}, and 42%, respectively, at the surface layer of Station C1; 0.03 ms^{-1}, 0.08 ms^{-1}, and 33%, respectively, at the bottom layer of Station C1; 0.01ms^{-1}, 0.10 ms^{-1} and 94%, respectively, at the surface layer of Station C2; 0.03, 0.07 ms^{-1}, and 52%, respectively, at the bottom layer of Station C2. The main discrepancies occurred during the slack period. Overall, the model satisfactorily reproduced the variations of water currents during the summer of 1987.

4.3. Salinity

The salinity calibration period was from 5/1/2006 to 12/31/2006. The distributions of wind, non-tidal water level at the river mouth, and river discharge during the simulation period are shown in Fig. 4. The background diffusivity was calibrated to obtain better results. It was shown that a background diffusivity of $4.0\times10^{-5}m^2s^{-2}$ resulted in a reasonable agreement. A comparison between the model results and measurements is shown in Fig. 5

The salinity shows large variations in responding to the variations of water level and river discharge. A water level rise at Day 38.7 resulted in a salinity increase in the whole estuary. A large river discharge event occurred around Day 60 and diluted the estuary significantly. Another tremendous salinity increase happened before the tropical storm Ernesto on September 1, 2006 (Day 123), which was mostly induced by a month long

period of extremely low river inflow. The salinity decreased quickly as freshwater discharge increased after Day 122. Due to the lack of daily observed salinity data at the open boundary, the modeled results could not be expected to represent the complete history of salinity variations in the estuary. Generally, the modeled salinities agreed with the measured data. The model was able to catch salinity variations and vertical stratification (Fig. 5). Overall, the model results are unbiased (Fig. 6) and are acceptable.

5. Model results

5.1. The effects of down-estuary and up-estuary winds

The temporal and spatial variations of WA depend on the freshwater discharges, wind, and tidal forcing conditions. WA under a realistic forcing condition was simulated by using real observation data (E00). An example of vertically averaged WA variation at Station 3 from Day 120 to 240 is shown in Fig.7 (see Fig. 1 for station location). WA varied between 70 to 125 days during the simulation period. WA increased from Day 120 to Day 190 and it decreased significantly from Day 200 to 210. A large fluctuation occurred around Day 205. WA oscillated continuously from Day 210 to 290.

Wind contributes greatly to the estuarine circulation in the Chesapeake Bay. Previous investigations suggest that wind energy peaks at 8 and 3.5 days in this area (Wang, 1979). To diagnose the effect of wind on WA, experiments E01 (without wind), E02 (with intermittent down-estuary wind components), and E03 (intermittent up-estuary wind components) were conducted. The time series of WA variations at Station 3 for the experiments are shown in Fig.7. The results show that WA fluctuated in a similar pattern for all the simulations. This suggests that river flow contributed to WA variation to a

large extent. In general up-estuary winds increased WA while down-estuary winds decreased WA. The results are consistent with the findings of Shen and Wang (2007). Before Day 178, WA of the Real Case (E00) was similar to that with up-estuary wind components, indicating the importance of up-estuary winds in affecting transport timescale. Although the intermittent up-estuary wind components were forced in the experiment, an accumulative effect was evident, which will be further discussed. After Day 205, the down-estuary wind played a more important role in altering WA as river discharge increased. An increased WA was evident from Days 190 to 200 under up-estuary wind forcing.

The spatial distributions of vertically-averaged (averaged from Day 192 to 193) WA in the estuary are shown in Fig. 8. For the case without wind forcing, it took about 140 days for the tracer released at the headwater to be transported out of the estuary (Fig. 8a). The down-estuary wind generally reduced the transport time in the estuary (Fig. 8b). The tracer needed about 130 days to escape from the estuary. WA decreased by 2.48% on average over the whole estuary. In contrast, the up-estuary wind increased WA significantly (Fig. 8c). It took more than 150 days for the tracer to travel from the headwater to the river mouth. WA increased by 10.65 % on average in the estuary.

The distribution of WA depends highly on the gravitational circulation (Shen and Lin, 2006). The vertical distributions of 25-hour tidally averaged salinity and WA along the longitudinal transect is shown in Fig.9. It can be seen that the down-estuary wind generally increased the buoyancy-induced circulation (Fig. 9b). Salt intrusion moved farther upstream and stratification increased in the region from 60 to 90 km, which is consistent with the enhanced gravitational circulation. In contrast, under up-estuary wind

forcing, WA increased about 30 days near the mouth of the estuary compared to the cases with down-estuary wind forcings. It can be seen that the up-estuary wind reduced salt intrusion and the 1 ppt salinity contour moved 15 km downstream (Fig. 9c). WA increased in the segment from 60 to 110 km, where gravitational circulation was reduced (Figs. 9b and 9c). Sanay (2003) demonstrated that for a down-estuary wind forcing, buoyancy-induced circulation is enhanced. For a moderate up-estuary wind forcing, wind-driven circulation overwhelms buoyancy-induced circulation. This is consistent with the model results in this study. Our results also demonstrate that the influence of up-estuary wind on the transport timescale of dissolved substances is stronger than the down-estuary wind. This complies with the pattern found in the Chesapeake Bay (Shen and Wang, 2007).

A noticeable feature of WA distribution is the lateral variation. Under the buoyancy force, WA at the western side of the River (i.e, the right hand side facing downstream) was generally lower than that near the eastern side. This can be attributed to the bathymetry, Coriolis force, and tidal asymmetries (Shen and Haas, 2004). The down-estuary wind enhanced the buoyancy-induced lateral variations of non-tidal current and WA while the moderate up-estuary wind could change the lateral distribution of longitudinal non-tidal flow and thus alter the lateral variation of WA. An example of the lateral non-tidal current and WA distributions at a selected Section 1 from Day 238 to 240 are shown in Fig. 10. Without the wind forcing, the downstream current was biased at the surface of the western side while the upstream current was located at the bottom (Fig. 10d). WA at the western side of the river was lower than that at the eastern side (Fig.10g). The down-estuary wind slightly enhanced the estuarine circulation. The

isohalines were vertically distributed and the lateral gradient of salinity was increased whereas the stratification pattern was identical with the case without wind forcing. The lateral asymmetric distribution of WA with an overall reduction of WA was similar to the situation without wind. In contrast, the up-estuary wind changed the estuarine circulation more apparently. It generated a lateral pattern with upstream flows located in the side shoals and downstream flows located in the channel at Section 1(Fig. 10f). The lateral distribution of WA was altered correspondingly (Fig. 10i): the lower WA occurred in the channel while higher WA was present along the side shoals.

5.2. The local and non-local wind effect

Water motions in a tributary can be induced by both the local and non-local winds through coupling with a neighboring large estuary. Non-local wind often causes sea level fluctuations in the Rappahannock River (Fig. 4). The influences of wind on the WA can be distinguished as the local and non-local wind effects. The former acts directly on the surface of the waterbody and the latter influences the estuary through wind-induced sub-tidal variations at the river mouth. Experiments E31-E33 were conducted to diagnose the local and non-local wind effects on WA.

Because WA varied during the model simulation, the results averaged over the last 2 days of the simulations were selected for analysis. For the Real Case simulation, it took approximately 130 days for the tracer released at the headwater to be transported to the river mouth (Fig. 11a). Because setup dominated the variation of subtidal water level during the simulation period (Fig. 4), excluding setup at the river mouth would enhance downstream transport, thus decreasing WA. Without non-local wind forcing, WA

decreased but the root mean square (RMS) difference between the simulations with and without non-local wind is only 2.64 days in the estuary. The WA distribution shares a similar pattern with the results of the Real Case. However, without local wind forcing, WA in the estuary became much different from that of the Real Case (Fig. 11b). The RMS difference of WA increased to 28.32 days between the simulations with and without local wind forcing. Without local wind forcing, the lateral differentiation increased, WA decreased near the western shoreline but increased near the eastern shoreline. This clearly indicates the effect of local wind on the spatial distribution of WA.

To further examine the local and non-local wind effects on WA, the time series of WA at two stations (Stations 1 and 3) are shown in Figs. 11c and 11d, respectively. The change of WA in response to the freshwater discharge was evident, especially at Station 1, which lies in the freshwater portion of the estuary. The influence of freshwater discharge on WA decreased downstream. WA increased up to 20 days with the local wind forcing in the estuary. It can be clearly seen that WA almost follows that of the Real Case without non-local wind while WA deviated from that of the Real Case more dramatically without the local wind. The increase of WA was less than 5 days during strong setup events (i.e., around Day 125, 160, 206, 227). Because the local wind has a much stronger impact on estuarine mixing, it alters WA more notably. The results indicate that the local wind effect is more important for long-term transport in the Chesapeake Bay tributaries under normal wind conditions.

5.3. Wind pulse effect

The model results show that the wind effect on WA is accumulative within a certain period even when wind forcing is periodic. The duration of the wind pulse effect is crucial for the transport processes in the estuary. A strong wind pulse can generate a strong perturbation to the estuary and alter the mixing and stratification pattern in estuaries. The response of WA to the wind pulse was examined by conducting simulations E21 and E22. We separated a wind pulse into two stages: (1) accelerating phase (from Day 200 to 201) when the wind speed increased; (2) decelerating period (from Day 201 to 202) when the wind speed decreased. During a storm event (such as a hurricane), the response of an estuary is basically barotropic (Gong et al., 2007; Li et al., 2007). During the acceleration phase, the wind induces either a flow pattern with downwind current at the water surface and upwind current at the bottom or a uni-directional downwind flow depending on the mixing, and establishes a horizontal water level slope against the wind forcing. During the deceleration stage, the established barotropic gradient drives an upwind flow in the water column. After the passage of a storm event, the estuary readjusts itself, enduring oscillations for both elevation and current. For the wind pulse simulations, the maximum wind speed was 15 $m \cdot s^{-1}$ and the maximum W_e was calculated as 10.92, showing a dominant effect of wind forcing relative to the buoyancy effect.

The downstream wind, compared with the data without wind (Fig.12a), generated a strong downstream current at Station 1 and enhanced estuarine circulation in the region downstream of Station 2 during the acceleration phase (Fig. 12b).The up-estuary wind induced an upstream current at the surface layer and a downstream current at the bottom layer in the region downstream of Station 2. The changes in current and mixing altered

the tracer transport and WA. The strong mixing induced by the wind pulse destratified the vertical WA distribution. The down-estuary wind pushed the WA contour downstream, thus decreasing WA in the estuary, while the up-estuary wind induced an opposite effect.

During the deceleration phase, the surface gradient established during the acceleration phase generated a reverse flow in the estuary. Large upstream currents were developed at the subsurface and middle layers in the water column for the down-estuary wind while a strong downstream current was observed for the up-estuary wind. For the down-estuary wind, the vertical distribution WA became more stratified (Fig. 12e). The bottom WA increased while the surface WA decreased compared to that without wind in the region downstream of Station 2. For the up-estuary wind, WA contour was advected downstream and WA was generally higher than that without wind (Fig. 12f).

After the passage of the wind pulse, the vertical distribution of WA for both cases of down-estuary and up-estuary wind pulses became similar to that without wind. For the down-estuary wind pulse, WA upstream of Station 2 was higher than that without wind while WA was lower downstream of Station 2 (Fig. 12h). For the up-estuary wind pulse, WA adjusted quickly (Fig.12i). A time series plot of the perturbation and recovery processes at Station 4 are shown in Fig.13. It can be seen that WA changed in 3 days for a 2-day period wind pulse and WA returned to a without wind status at approximately Day 240, which was 40 days for the adjustment.

Overall, the influence of wind pulse on WA is more pronounced downstream in the estuary where stratification persists. A wind pulse for a 2-day period can impact WA and the influence lasts up to 40 days. As the wind pulse can alter the mixing, stratification and

estuarine circulation in an estuary, the adjustment time is longer in the deeper area, such as Station 4 (Fig. 13), as demonstrated by MacCready (1999). The results suggested that an accumulative effect can be expected for the tributaries of the Chesapeake Bay, which experiences consecutive wind events with a dominant period of 2-10 days.

6. Discussion

Model simulations under different wind forcing conditions suggested that wind has a significant influence on the estuary gravitational circulation, upon which WA highly depends. Hansen and Rattray (1965) obtained the estuarine circulation pattern by using a steady-state approach:

$$u(z) = \frac{1}{48}\frac{g\frac{\partial \rho}{\partial x}h^3}{\rho K}\left[1-9\left(\frac{z}{h}\right)^2-8\left(\frac{z}{h}\right)^3\right]+\frac{3}{2}u_0\left[1-\left(\frac{z}{h}\right)^2\right]$$

$$+\frac{1}{4}\frac{\tau_s h}{\rho K_m}\left[1+\frac{z}{h}+3\left(\frac{z}{h}\right)^2\right] \qquad (6)$$

where K_m is the eddy viscosity, and u_0 is the mean outflow due to river discharge. The first two terms of Eq. (6) describes the estuarine circulation without wind forcing and the last term represents the circulation induced by the wind effect. It can be seen that the gravitational circulation will be strengthened with constant down-estuary wind. When wind becomes up-estuary, the wind-induced current can reduce the estuarine circulation. It can cause inflow at the surface and outflow at the middle layer (Geyer, 1997). Our model simulations (E01-E03) agree with the circulation pattern obtained by Eq. (6) under continuously varying wind conditions. The up-estuary wind forcing weakens the

estuarine circulation and reduces outflow, resulting in an increase in transport time. Under down-estuary wind forcing, the estuarine circulation undergoes minor changes and the decrease in transport time is not significant.

Many studies suggest that the influence of wind on stratification depends highly on the precondition of the estuary stratification. The competition between wind and buoyancy force can be represented by the Wedderburn number. When buoyancy forcing becomes stronger (smaller Wedderburn number situations), the wind effect on transport timescale is reduced given the same magnitude of wind forcing. To understand the competition between wind and buoyancy forces and their influence on transport timescale, we conducted model simulations under constant (with a velocity of 5 $m \cdot s^{-1}$) down-estuary and up-estuary wind forcing (Experiments E31-E33 and E41-E43). Although wind forcing changes continuously in magnitude and direction in a real situation, the model results under constant wind forcing can be considered as an extreme case that provide measures for the maximum deviation of transport timescale that can be expected. These results can be further compared with estuary circulation derived from a steady-state approach.

For the experiments E31-E33, river discharge was specified as constant mean flow. Under mean flow condition, $W_e = \pm 0.77$, representing a moderate wind effect in respect to the buoyancy effect (plus sign signifies the down-estuary wind situation). For the baseline condition (E31), it took about 160 days for the tracer released at the headwater to be transported out of the estuary (Fig. 14a). Under the down-estuary wind (Fig. 14b), the tracer took about 150 days to escape from the estuary. WA decreased 6.13% on average over the whole estuary. Conversely, the up-estuary wind increased WA significantly (Fig.

14c). It took about 210 days for the tracer to be transported from the headwater to the river mouth, a 50 day increase compared to the baseline condition. WA increased 19.42% on average in the estuary. These results agree with those of experiments E01-E03.

Under high flow conditions (Experiments E21-E23), W_e is reduced to 0.59. With high river discharge, WA at the estuary decreased greatly compared to the baseline condition (Fig. 15a). It took less than 60 days for the tracer to be transported out of the estuary. The down-estuary wind reduced WA overall. It took less than 50 days for the tracer to be transported from the headwater to the mouth (Fig. 15b). The down-estuary wind reduced WA by 13.96% (note WA decreased by 6.13% under the mean flow condition) on average in the estuary. With an increase of buoyancy force under a high flow condition, the pre-status of stratification can be expected to be less altered by wind forcing. For the up-estuary wind, WA at the river mouth increased by 10 days (Fig.15c). The increase of transport time was much less than that under the mean flow condition, which is 50 days. The up-estuary wind increases WA by 13.97% (note WA increasd by 19.42% under the mean flow condition) on average in the estuary. This suggests that the impact of wind forcing on the transport timescale depends highly on the competition between the wind induced mixing and the stratification established under the buoyancy forcing of the freshwater discharge. As high flow inputs large buoyancy to the estuary and results in the establishment of strong estuarine circulation in the Mesohaline region, the wind forcing is not strong enough to change the estuarine stratification status significantly even though the up-estuary wind increases vertical mixing. This effect can also be observed from the model simulation using real-time data (simulations E00-E12). The local wind effect was reduced when the estuary endures high inflow after Day 200 (Fig. 11).

Since the wind pulses usually occur intermittently or continuously in a real situation, studying a single wind pulse has limitations. An alternative is to use multiple wind pulses in the study. But it would be difficult to isolate the effect of a specific wind pulse. In this study, we diagnosed the influence of an isolated wind event on the transport timescale and examined its recovery time. If a perturbation generated by an energetic wind event only lasts for a short period, its contribution to the long-term transport can be considered insignificant. On the other hand, if a wind generated perturbation persists in the system for a long period, the accumulative effect is important. Our model results forced by intermittent up-estuary or down-estuary winds (E02-E03) indicate that the up-estuary wind effect is accumulative, persistent and plays a dominant role for controlling estuarine transport timescale.

Our model results show that the down-estuary wind reduces WA in the whole estuary. This is different from Gustafsson and Bendtsen (2007) but is consistent with Shen and Wang (2007). The increase of WA under down-estuary wind in Gustafsson and Bendtsen (2007) could be due to the large Wedderburn number and thus the decrease of estuarine circulation in their study.

7. Summary

WA provides a good measure for transport timescale of dissolved substances in estuaries. Besides the influence of tidal variation and river discharge, wind also affects WA significantly. Wind plays an important role in regulating mixing, stratification, salt transport, and estuarine circulation in estuaries. Therefore, it has a great impact on the transport timescale in estuaries.

The effects of wind on transport timescale depend strongly on the competition between the wind forcing and buoyancy forcing. The pre-status of the estuarine circulation can also alter the effect of wind forcing. The down-estuary wind generally decreases WA along the estuary. Because the stratification persists in the Rappahannock River, a decrease in WA due to down-estuary wind is marginal. The up-estuary wind produces the opposite impact on WA and has a more important impact on age distribution as it changes estuarine circulation more significantly. For a situation in which wind forcing dominates over buoyancy forcing, the up-estuary wind causes greater changes in WA than that of the down-estuary wind. As buoyancy forcing increases under high river discharge, the effect of up-estuary wind decreases.

In general, the lateral age distribution is more biased towards the right side of the estuary when looking downstream. Such an asymmetric pattern is due to the asymmetric lateral variation of net circulation. However, this pattern can be changed by the up-estuary wind forcing. The interaction of up-estuary winds and geometry can alter the lateral circulation, resulting in a more symmetric pattern in the lower estuary.

Wind pulse can impose great disturbances on the non-tidal circulation and stratification in the estuary, thus affecting WA in a certain period of time. Our model results show that a 2-day period wind pulse with a peak velocity of 15 ms^{-1} can change WA by approximately 3 days and its influence can last for up to 40 days. The simulation, forced only by real up-estuary wind components, indicates that the influence of up-estuary wind persists in the system and represents a significant contribution to the transport timescale.

The model experiments suggest that the setup and setdown of water level imposed at the river mouth due to remote wind effect has a weak impact on WA under normal wind

conditions. The local wind has a significant impact on WA distribution as it directly changes the vertical mixing and subsequent estuarine circulation.

Acknowledgement

The authors would like to thank for Dr. Albert Y. Kuo for his constructive suggestions. This is contribution number ×× from the Virginia Institute of Marine Science, School of Marine Science, College of William and Mary, Virginia. The first author was supported by the "one-hundred-scholar" program of Sun Yat-sen University, China.

References

Bolin, B., Rodhe, H., 1973. A note on the concepts of age distribution and transit time in natural reservoirs. Tellus 25, 58-63.

Boynton, W.R., Garber, J.H., Summers, R., Kemp, W.M., 1995. Inputs, transformations, and transport of nitrogen and phosphorus in Chesapeake Bay and selected tributaries. Estuaries 18, 285-314.

Delhez, E.J.M., Deleersnijder, E., 2002. The concept of age in marine modeling, II. Concentration distribution function in the English Channel and the North Sea. Journal of Marine Systems 31, 279-297.

Deleersnijder, E., Campin, J.M., Delhez, E.J.M., 2001. The concept of age in marine modeling. I. Theory and preliminary model results. Journal of Marine Systems 28, 229-267.

Delhez, E.J.M., Campin, J.-M., Hirst, A.C., Deleersnijder, E., 1999. Toward a general theory of the age in ocean modeling. Ocean Modeling 1, 17-27.

Elliott, A.J., 1976. Response of the Patuxent Estuary to a winter storm. Chesapeake Science 17(3), 212-216.

Elliott, A.J., 1978. Observations of the meteorologically induced circulation in the Potomac estuary. Estuarine, Coastal and Marine Science *6*, 165-174.

Friedrichs, C.T., Hamrick, J.M., 1996. Effects of channel geometry on cross-sectional variation in along-channel velocity in partially stratified estuaries. Aubrey, D.G. and C.T., Friedrichs (Eds.) Buoyancy effects on coastal estuarine dynamics, Coastal and Estuarine Studies, American Geophysical Union, Vol. 53, 283-300

Galperin, B., Kantha, L.H., Hassid, S., Rosati, A., 1988. A quasi-equilibrium turbulent energy model for geophysical flows. Journal of Atmospheric Science 45, 55-62

Geyer, W.R., 1997. Influence of wind on dynamics and flushing of shallow estuaries. Estuarine, Coastal and Shelf Science 44, 713-722.

Gong, W., Shen, J., Reay, W.G., 2007. The hydrodynamic response of the York River estuary to Tropical Cyclone Isabel, 2003. Estuarine, Coastal and Shelf Science 73, 695-710.

Guo, X., Valle-Levinson, A., 2008. Wind effects on the lateral structure of density-driven circulation in Chesapeake Bay. Continental Shelf Research 28(17), 2450-2471.

Gustafsson, K.E., Bendtsen, J., 2007. Elucidating the dynamics and mixing agents of a shallow fjord through age tracer modeling. Estuarine, Coastal and Shelf Science 74(4), 641-654.

Hamrick, J.M., 1992. A Three-Dimensional Environmental Fluid Dynamics Computer Code: Theoretical and Computational Aspects. Special Report in Applied Marine Science and Ocean Engineering. No. 317 College of William and Mary, VIMS, 63pp.

Hamrick, J.M., Wu, T.S., 1997. Computational design and optimization of the EFDC/HEM3D surface water hydrodynamic and eutrophication models. In: Delich, G., Wheeler, M.F., (Eds.), Next Generation Environmental Models and Computational Methods. Society for Industrial and Applied Mathematics, Pennsylvania, pp. 143-161.

Hansen, D.V., Rattray, M. Jr., 1965. Gravitational circulation in straits and estuaries. Journal of Marine Research 23, 104-122.

Kuo, A.Y., Nelson, B.J., 1987. Hypoxia and salinity in Virginia estuaries. Estuaries 10(4), 277-283.

Kuo, A.Y., Moustafa, M.Z., 1989. Hypoxia in the lower Rappahannock Estuary, SRAMSOE No. 302. VIMS, The College of William and Mary, VA. 75 pp.

Li, M., Zhong, L., Boicourt, W.C., Zhang, S., Zhang, D., 2007. Hurricane-induced destratification and restratification in a partially-mixed estuary. Journal of Marine Research 65, 169-192.

MacCready, P., 1999. Estuarine adjustment to changes in river flow and tidal mixing. Journal of Physical Oceanography 29, 708-726.

McCarthy, R.K., 1993. Residual currents in tidally dominated, well-mixed estuaries. Tellus 45A, 325-340.

Mellor, G.L., Yamada, T., 1982. Development of a turbulence closure model for geophysical fluid problems. Review of Geophysical and Space Physics 20, 851-875

Nixon, S.W., Ammerman, J.W., Atkinson, L.P., Berounsky, V.M., Billen, G., Boicourt, W.C., Boynton, W.R., Church, T. M., DiToro, D.M., Elmgren, R., Garber, J.H., Giblin, A.E., Jahnke, R.A., Owens, N.J.P., Pilson, M.E.Q., Seitzinger, S.P., 1996. The fate of nitrogen and phosphorus at the land-sea margin of the North Atlantic Ocean. Biogeochemistry, 35, 141-180.

North, E.W., Chao, S.-Y., Sanford, L.P., and Hood, R.R., 2004. The influence of wind and river pulses on an estuarine turbidity maximum: Numerical studies and field observations in Chesapeake Bay. Estuaries 27, 132-146.

Officer, C.B., 1976. Physical Oceanography of Estuaries and Associated Coastal Waters. Wiley, New York, 465 pp.

Park, K**.,** Kuo, A.Y., 1996. Effect of variation in vertical mixing on residual circulation in narrow, weakly nonlinear estuaries. In: Buoyancy Effects on Coastal and Estuarine Dynamics (D.G. Aubrey and C.T. Friedrichs, eds.), Coastal and Estuarine Studies 53, AGU, pp. 301-317.

Park, K., 1993. A model study of hydrodynamic and water quality characteristics of the Rappahannock Estuary, Virginia. Ph.D thesis of The College of William and Mary**,** pp.219.

Sanay, R., 2003. Wind-induced exchange in semi-enclosed basins. Ph.D. dissertation, Old Dominion University, pp. 86.

Sanford, L.P., Boicourt, W.C., 1990. Wind-forced salt intrusion into a tributary estuary. Journal of Geophysical Research 95 (C8), 13357-13371.

Scully, M.E., Friedrichs, C., Brubaker, J., 2005. Control of estuarine stratification and mixing by wind-induced straining of the estuarine density field. Estuaries 28(3), 321-326

Shen, J., Haas, L., 2004. Calculating age and residence time in the tidal York River using three-dimensional model experiments. Estuarine, Coastal and Shelf Science 61, 449-461.

Shen J., Lin, J., 2006. Modeling study of the influences of tide and stratification on age of water in the tidal James River. Estuarine, Coastal and Shelf Science 68(1-2), 101-112.

Shen J., Wang, H.V., 2007. Determining the age of water and long-term transport timescale of the Chesapeake Bay. Estuarine, Coastal and Shelf Science 74, 585-598.

Takeoka, H., 1984. Fundamental concepts of exchange and transport time scales in a coastal sea. Continental Shelf Research 3(3), 322-326

Wang, D.-P., Elliott, A.J., 1978. Non-tidal variability in the Chesapeake Bay and Potomac River: evidence for non-local forcing. Journal of Physical Oceanography *8*, 225-232.

Wang, D.-P., 1979. Subtidal sea level variations in the Chesapeake Bay and relations to atmospheric forcing. Journal of Geographic Research 9, 413-421.

Wong, K.-C., 1994. On the nature of transverse variability in a coastal plain estuary. Journal of Geophysical Research 99 (C7), 14209-14222

Wu, J., 1982. Wind-stress coefficients over sea surface from breeze to hurricane. Journal of Geophysical Research 87:9704– 9706.

Xia, M., Xie, L., Pietrafesa, L.J., 2007. Modeling of the Cape Fear River Estuary plume. Estuaries and Coasts 30(4), 698-709.

Yang, Z.Q., Hamrick, J.M., 2005. Optimal control of salinity boundary condition in a tidal model using a variational inverse method. Estuarine, Coastal and Shelf Science 62 (1-2), 13-24.

Zimmerman, J.T.F., 1976. Mixing and flushing of tidal embayments in the Western Dutch Wadden Sea, Part I: distribution of salinity and calculation of mixing time scales. Netherland Journal of Sea Research 10, 149-191.

Table 1: Model simulation experiments

Model simulation	Description	Simulation period	Wind forcing	River flow	Tidal condition	Salinities at the open boundary	Wedderburn number
E00	Real Case	5/1/2006 to 12/31/2006 (240 days)	Observed wind				
E01	Diagnose down-estuary and up-estuary wind forcing using observation data	5/1/2006 to 12/31/2006 (240 days)	No wind	Observed river flow	Observed water level	Observed salinity data	
E02			Down-estuary wind component only				
E03			Up-estuary wind component only				
E11	Without non-local wind effect	5/1/2006 to 12/31/2006 (240 days)	Observed wind	Observed river flow	Astronomic tide only	Observed salinity	
E12	Without local wind effect		No wind		Observed water level	Observed salinity	
E21	Up-estuary wind pulse	300 days	Southeasterly wind pulse from Day 200 to 202	Mean flow	Mean tide	14 and 16 psu were specified at the surface and bottom	-10.92
E22	Down-estuary wind pulse		Northwesterly wind pulse from Day 200 to 202	Mean flow	Mean tide	same as above	10.92
E31	Baseline condition	300 days	No wind	Mean flow	Mean tide (tidal range of 0.37m)	same as above	
E32	Constant down-estuary wind		Northwesterly wind of 5m/s	Mean flow	Mean tide	same as above	0.77
E33	Constant up-estuary wind		Southeasterly wind of 5m/s	Mean flow	Mean tide	same as above	-0.77
E41	High flow	280 days	No wind	High flow	Mean tide	The same as above	
E42			Northwesterly wind of 5 ms^{-1}	High flow	Mean tide	same as above	0.59
E43			Southeasterly wind of 5 ms^{-1}				-0.59

Figure captions

Figure 1. Map of the Rappahannock River and the locations of measurement stations of the Chesapeake Bay Program (Circles are salinity stations, rectangles are water current stations, triangles are locations selected for analysis, and longitudinal and lateral cross-sections for analysis).

Figure 2. Results of mean tidal range calibration along the estuary (Square denotes tidal table data; solid line is the model result).

Figure 3. Calibration results of water currents (cross represents measurements, solid line signifies model results).

Figure 4. Time series of wind forcing, non-tidal water level at the river mouth and river discharge at the headwater of the estuary from 5/1/2006 to 12/31/2006.

Figure 5. Salinity calibration at stations surveyed by the Chesapeake Bay Program (solid line signifies the modeled surface salinity, dashed line signifies the modeled bottom salinity, rectangular and circle are observations at surface and bottom);

Figure 6. Comparison between the modeled salinities and observations (Circles are bottom salinities, rectangles are surface salinities)

Figure 7. Comparison of WA variations at Station 3 under the real case (solid line); no wind (dotted line); with components of down-estuary wind only (dash-dotted line); with components of up-estuary wind only (dashed line).

Figure 8. Distributions of vertically averaged WA for (a) without wind; (b) down-estuary wind component; and (c) up-estuary wind component.

Figure 9. Longitudinal distributions of salinity, residual current, and WA along the main channel of the estuary. Let panel is salinity, middle panel is current, and right panel is WA (a, d, g: without wind; b,e,h: down-estuary wind, c,f,i: up-estuary wind)

Figure 10. The lateral distribution of salinity (left), non-tidal current (middle) and WA (right) at Section 1 for the cases of without wind (upper panel), with down-estuary wind component (middle panel) and with up-estuary wind component (bottom panel).

Figure 11. The distribution of vertically-averaged WA (a: with real wind (black line) vs. without non-local wind (red line); b: with real wind (black line) vs. without local wind effect (red line)) and time series of WA at selected stations with, and without local and non-local wind (c: at Station 1; d: at Station 3).

Figure 12. The distribution of non-tidal longitudinal current along the channel of the estuary and wind pulse induced change of WA. Left column (a, d, g) is the baseline condition, middle column (b, e, h) is the case with down-estuary wind pulse and right

column is the case with up-estuary wind pulse. The upper panel is during the acceleration period (a, b, c), the middle panel is during the deceleration period (d, e, f), and the lower panel is during the wind pulse succeeding period (g, h, i).

Figure 13. Time series of subtidal longitudinal current and wind pulse induced change of WA at Station 4.

Figure 14. The distribution of vertically-averaged WA under mean flow condition (a: without wind; b: with constant down-estuary wind; c: with constant up-estuary wind).

Figure 15. The distribution of vertically-averaged WA under high flow condition (a: without wind; b: with constant down-estuary wind; c: with constant up-estuary wind).

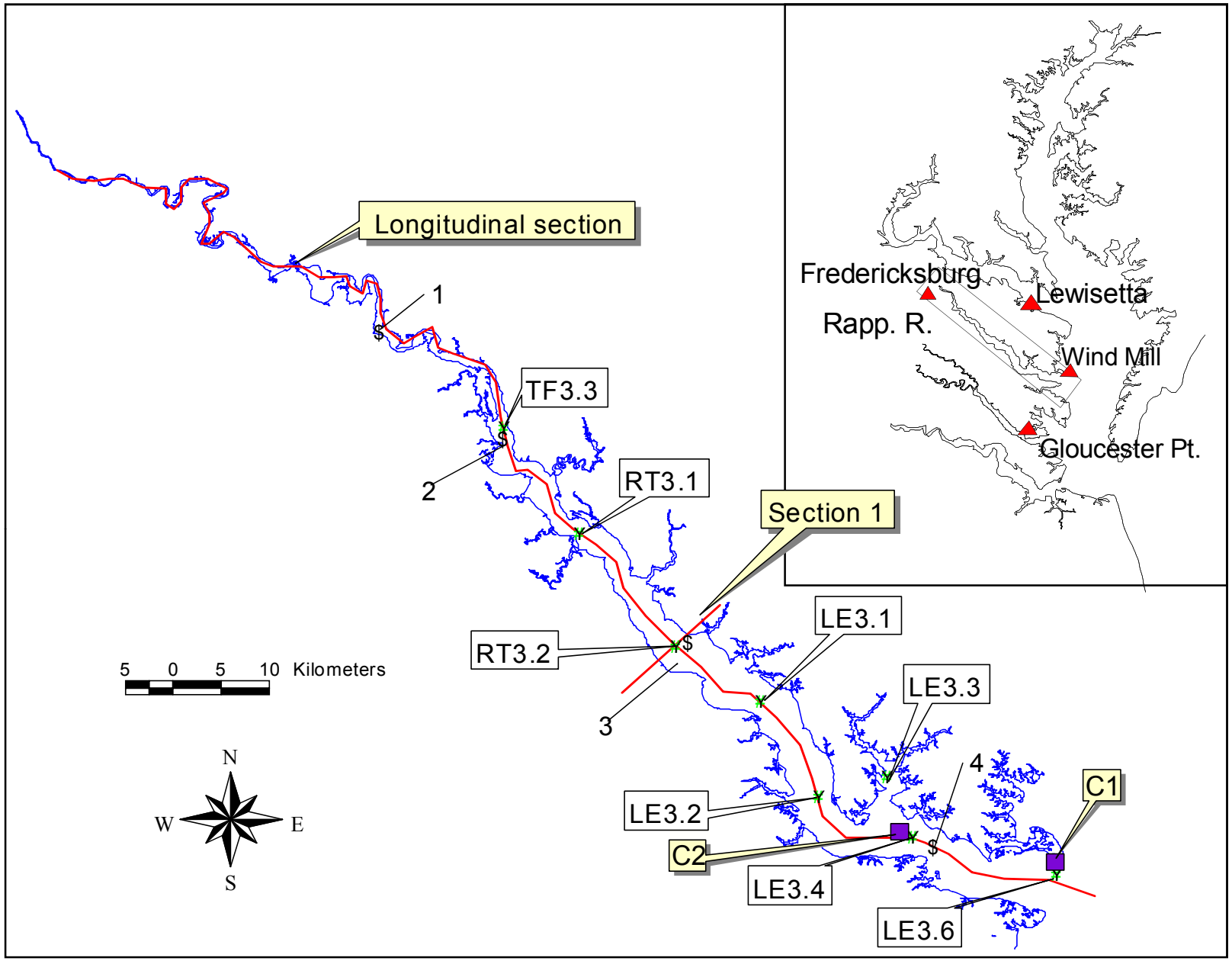

Fig. 1

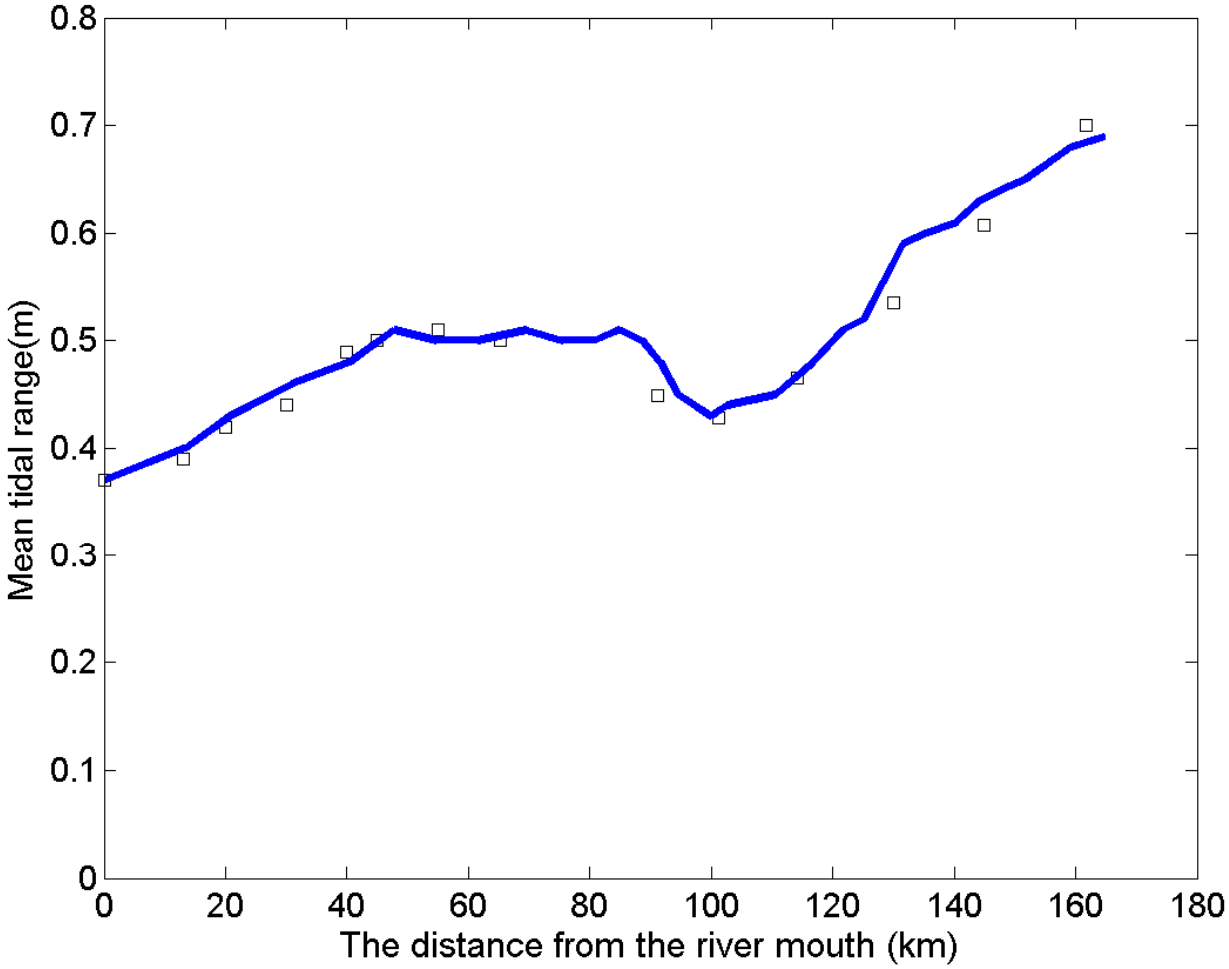

Figure 2

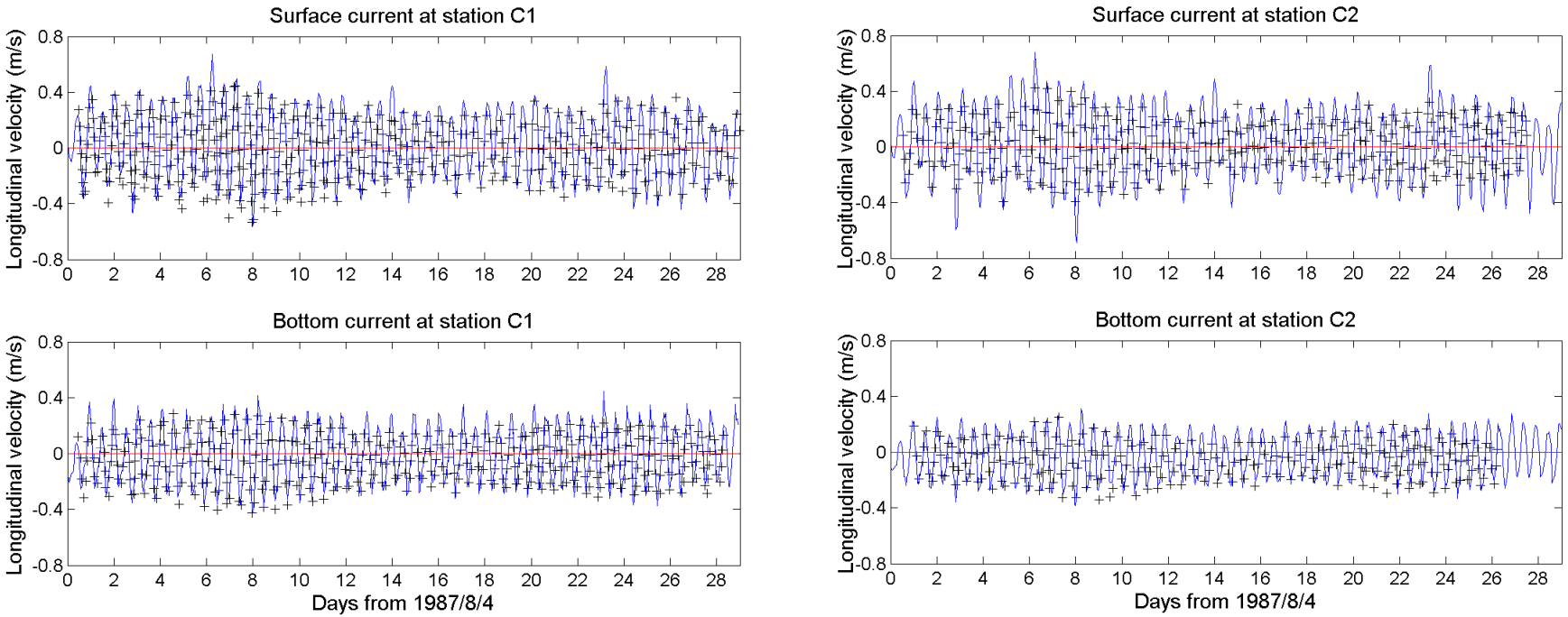

Figure 3

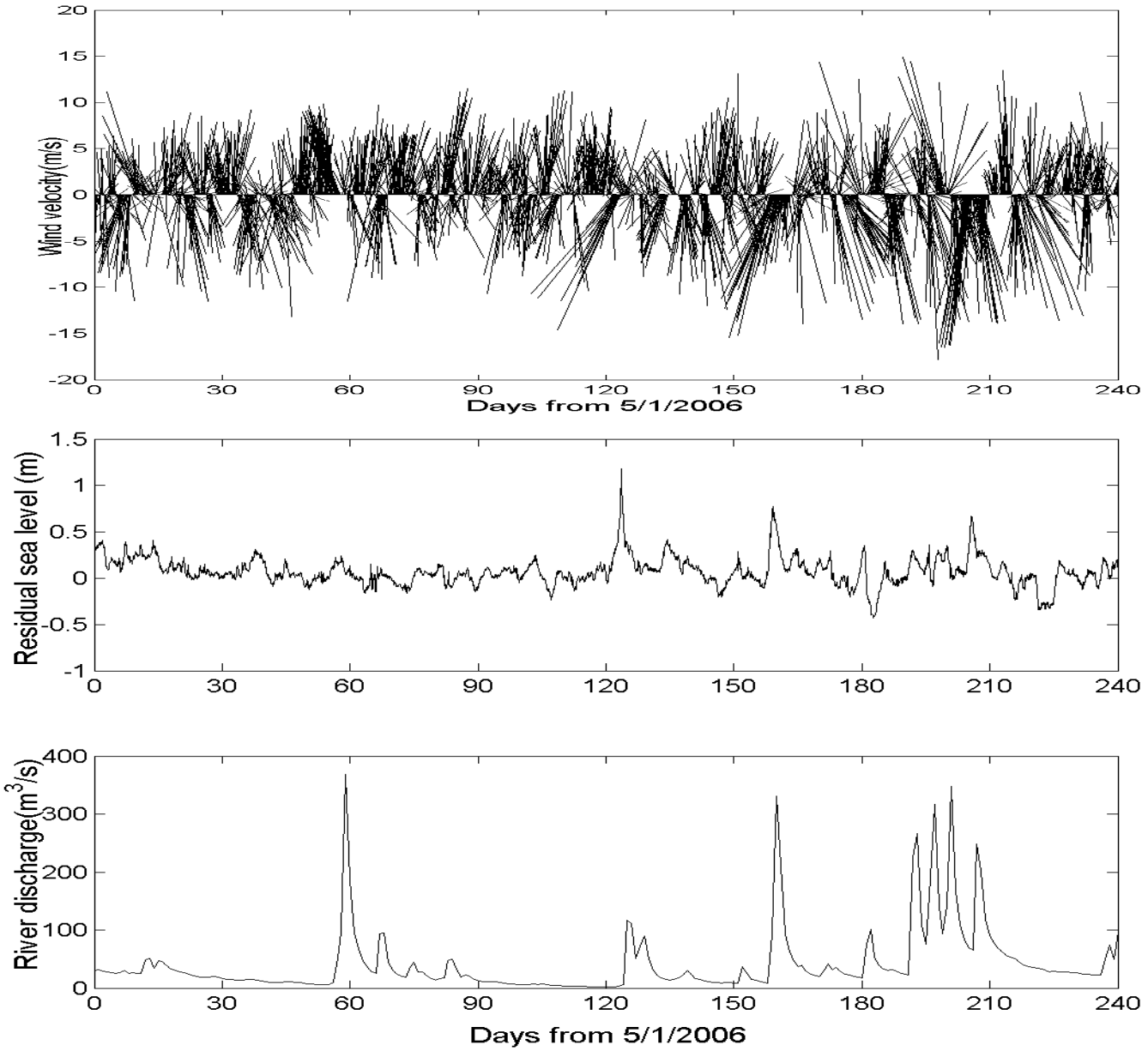

Figure 4

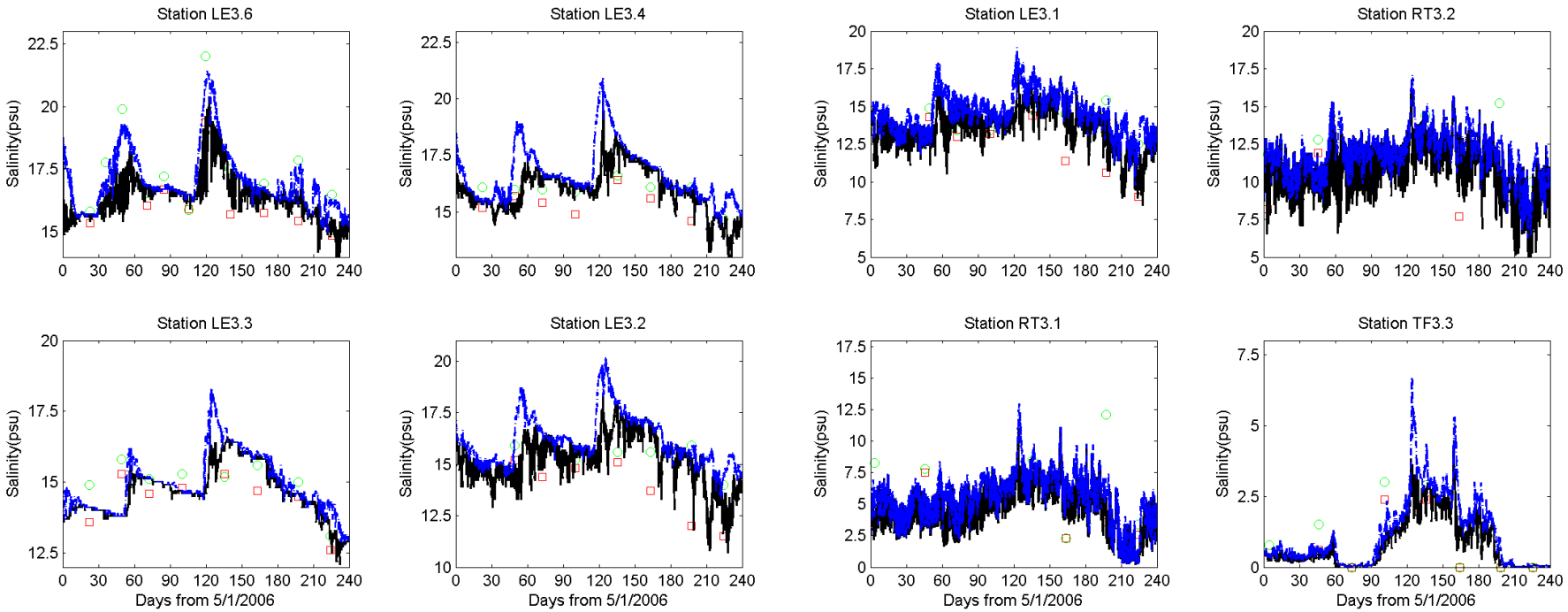

Figure 5

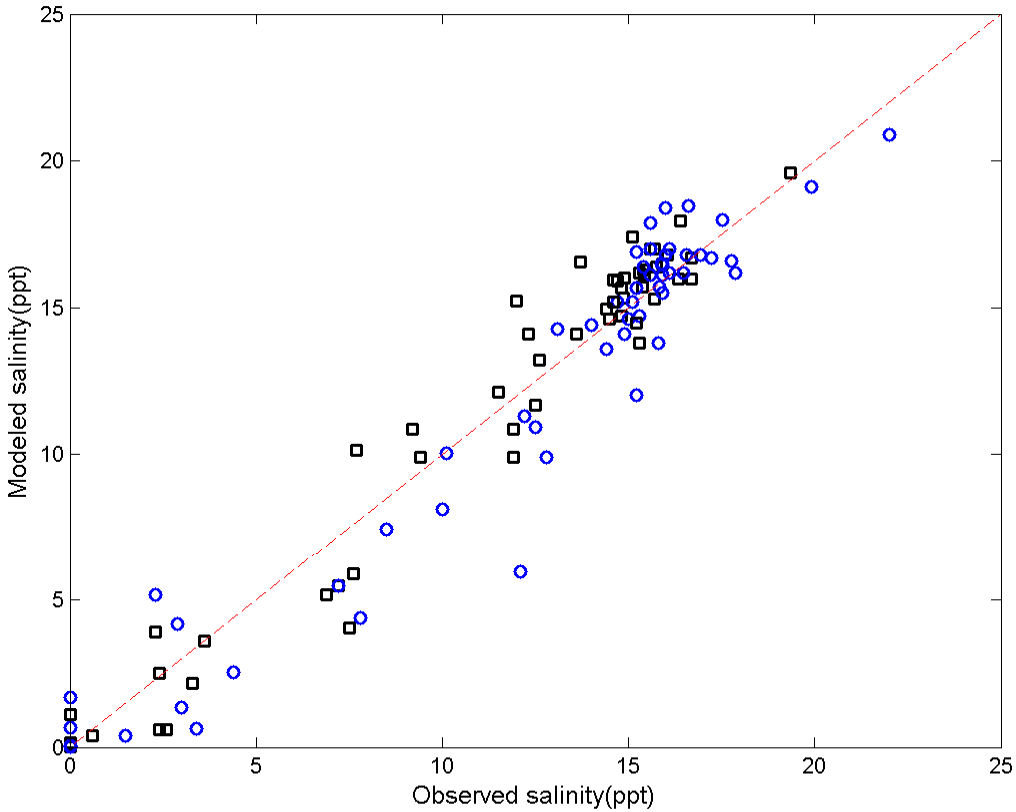

Figure 6

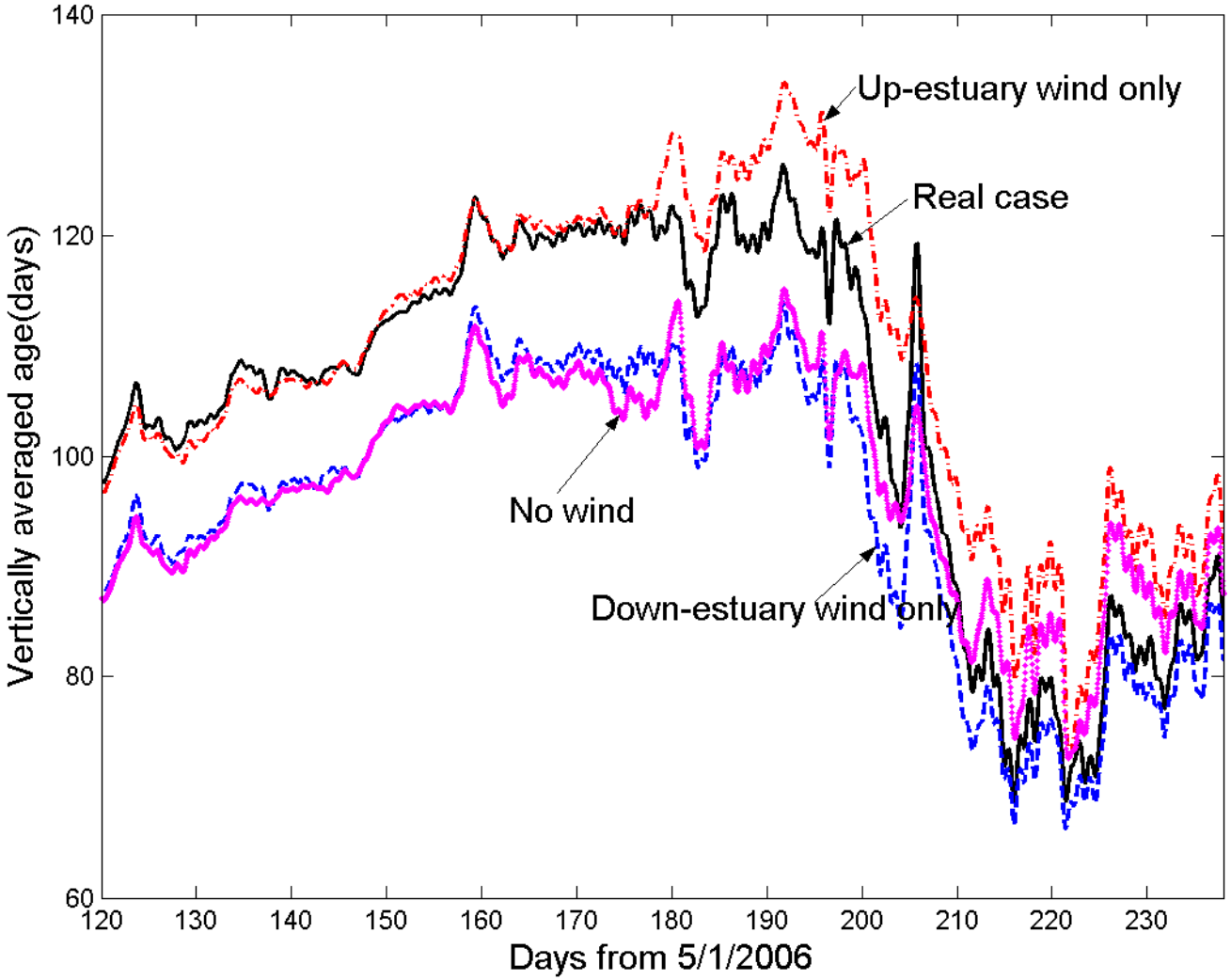

Figure 7

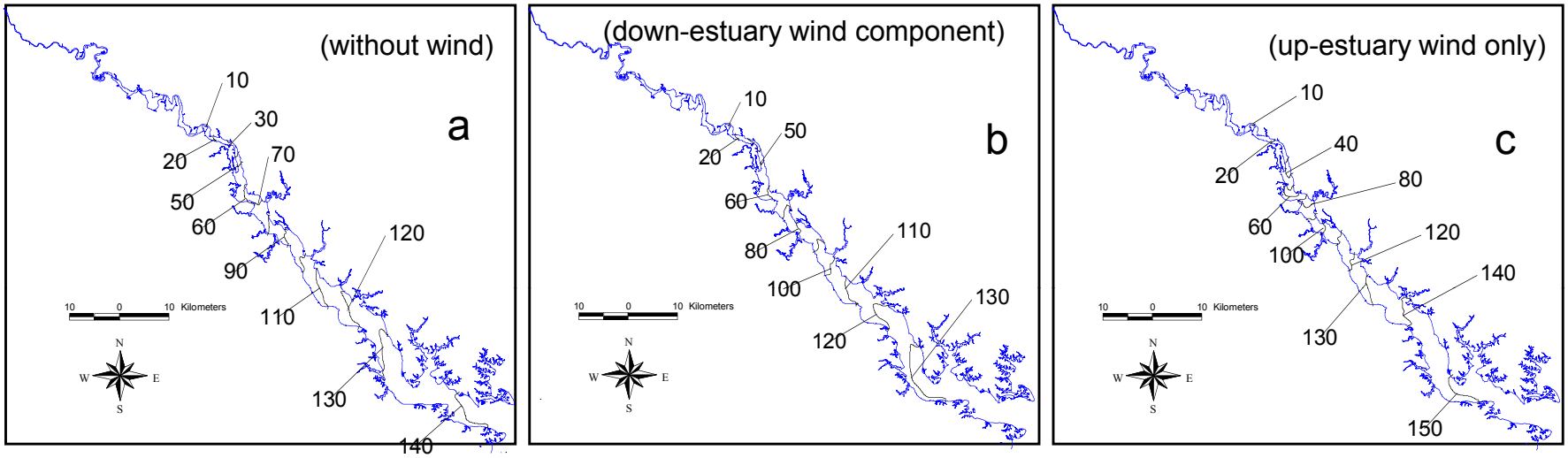

Figure 8

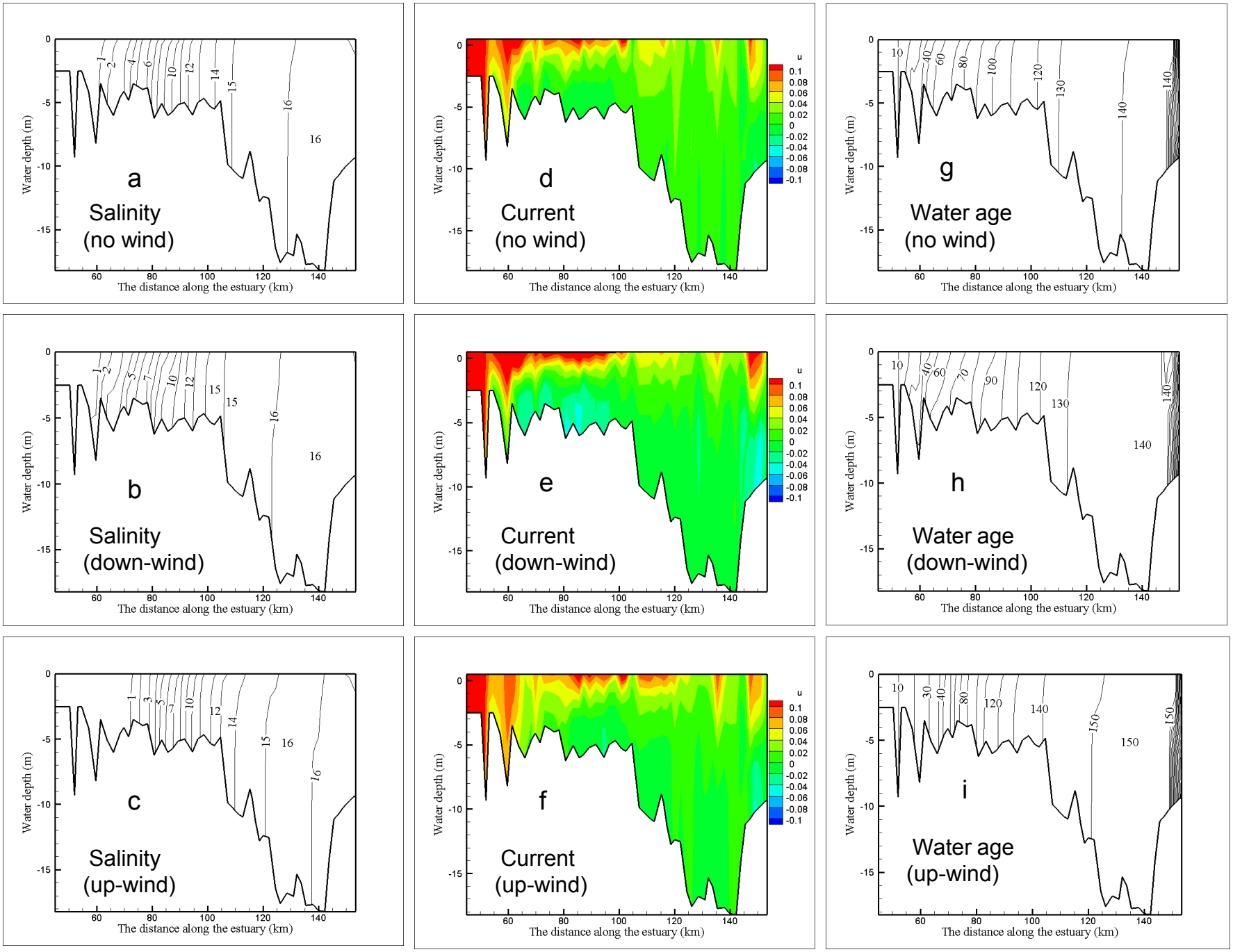

Figure 9

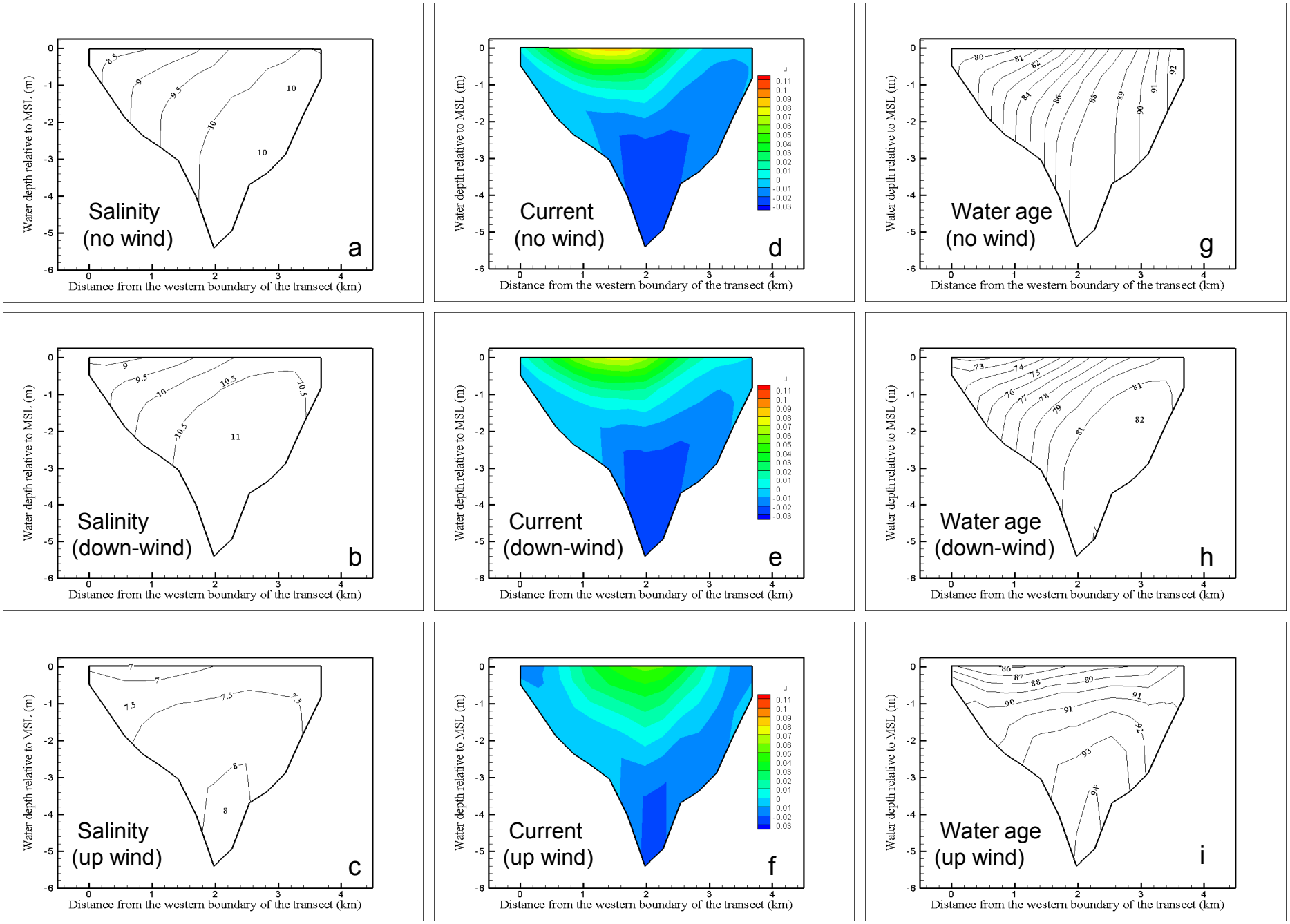

Figure 10

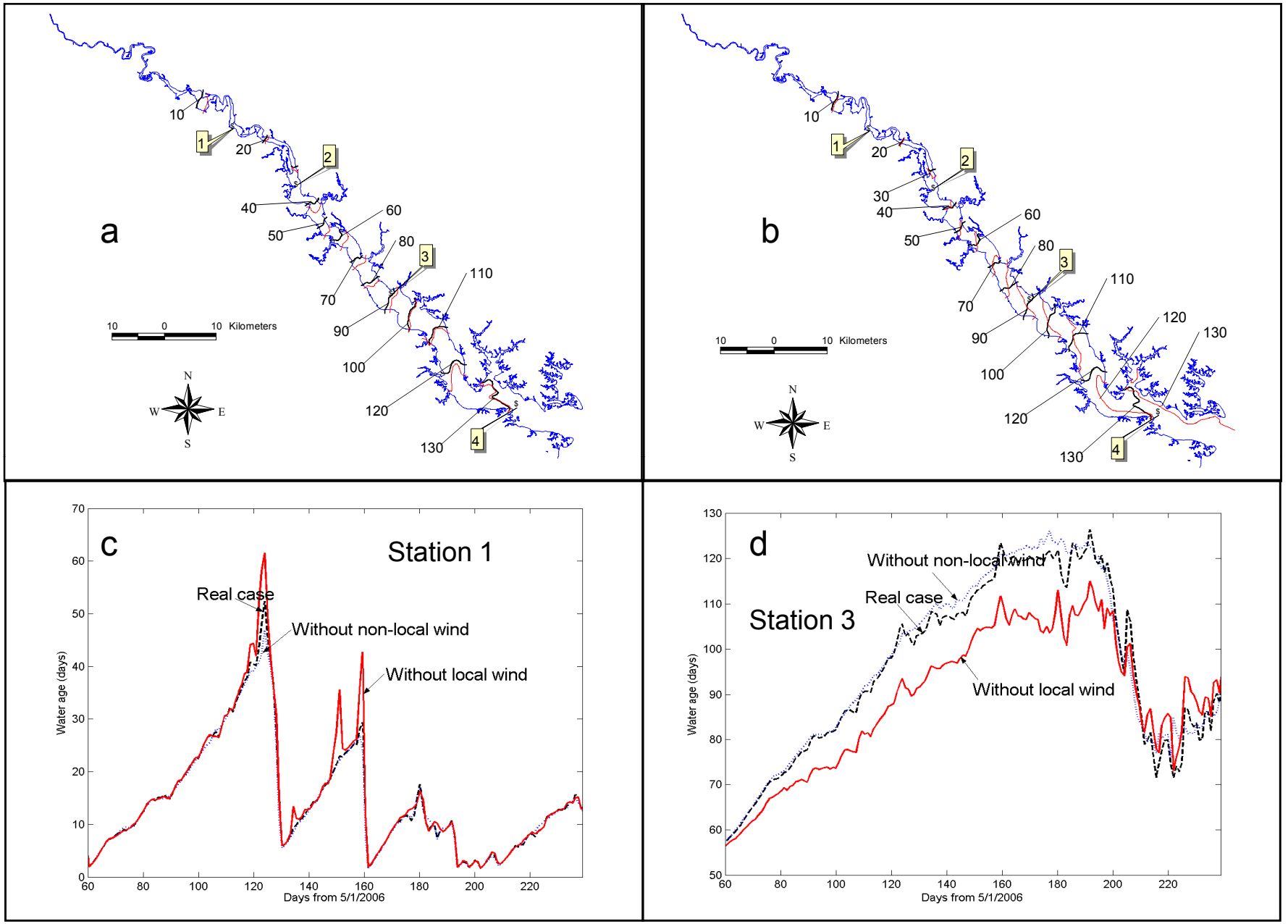

Figure 11

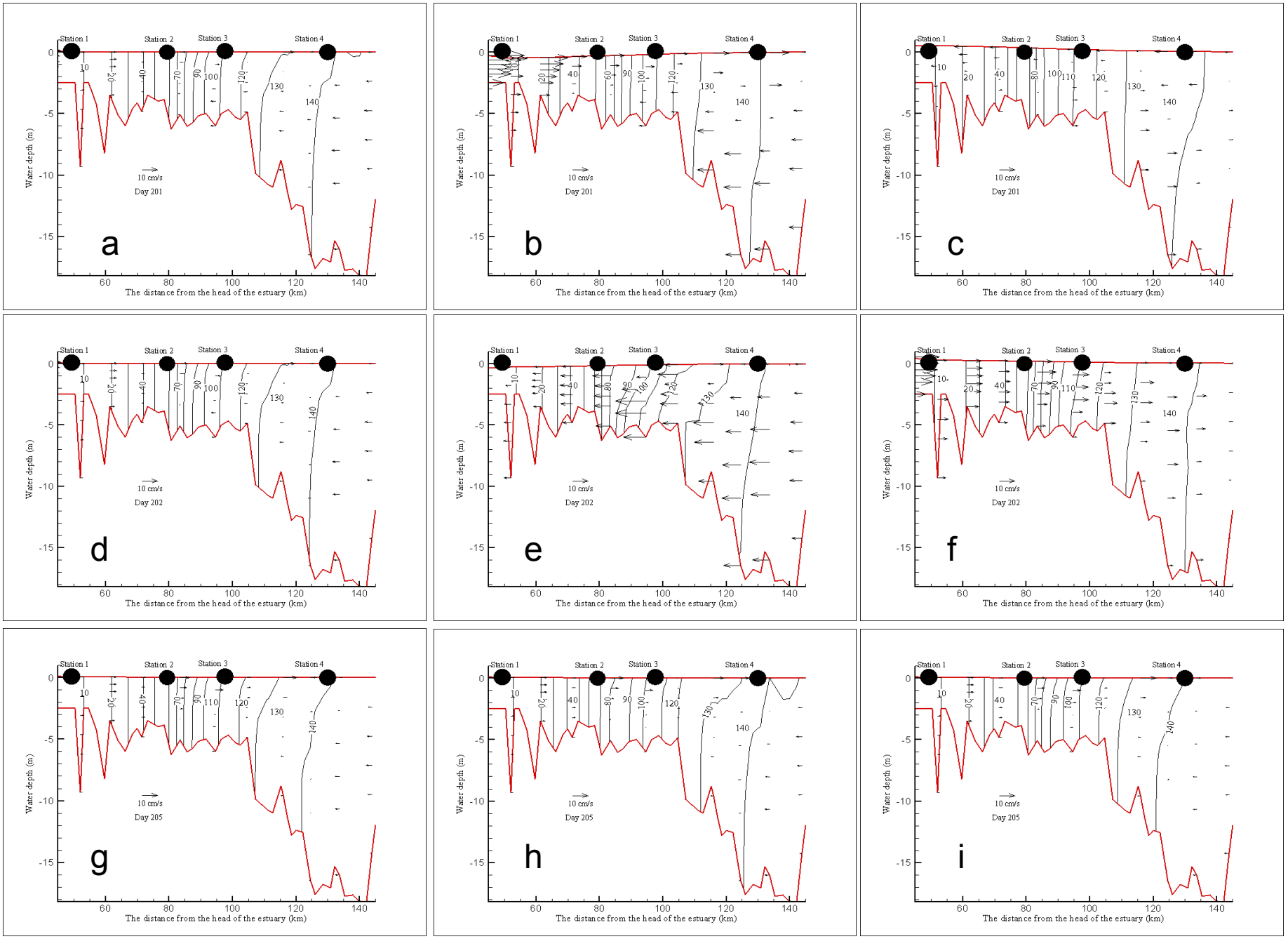

Figure 12

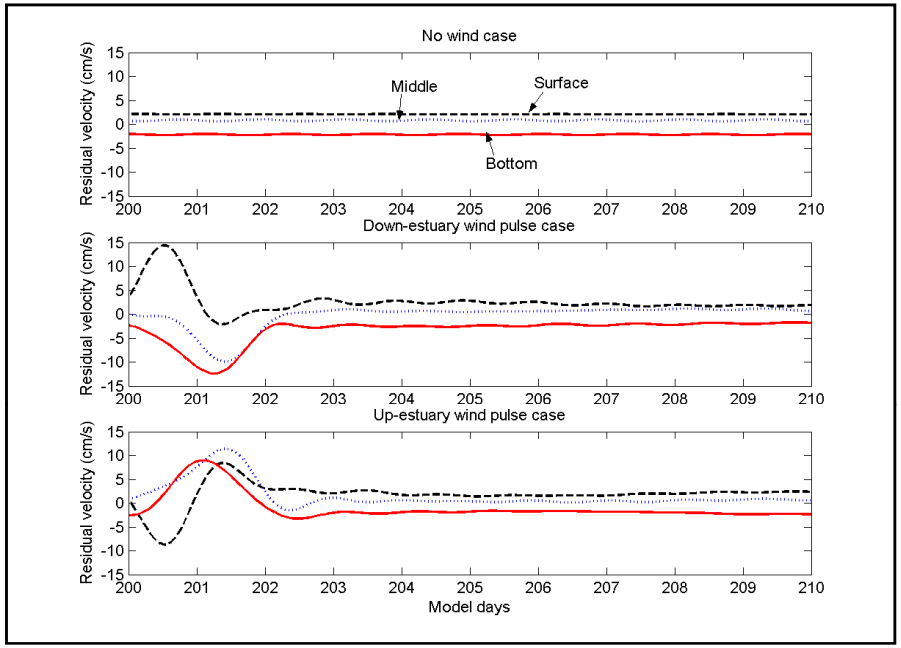

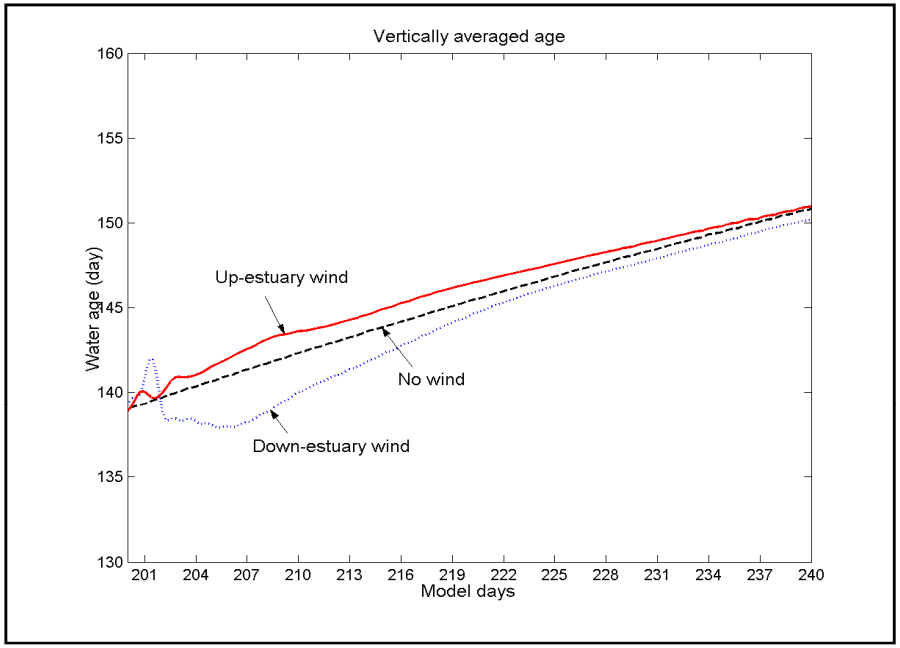

Figure 13

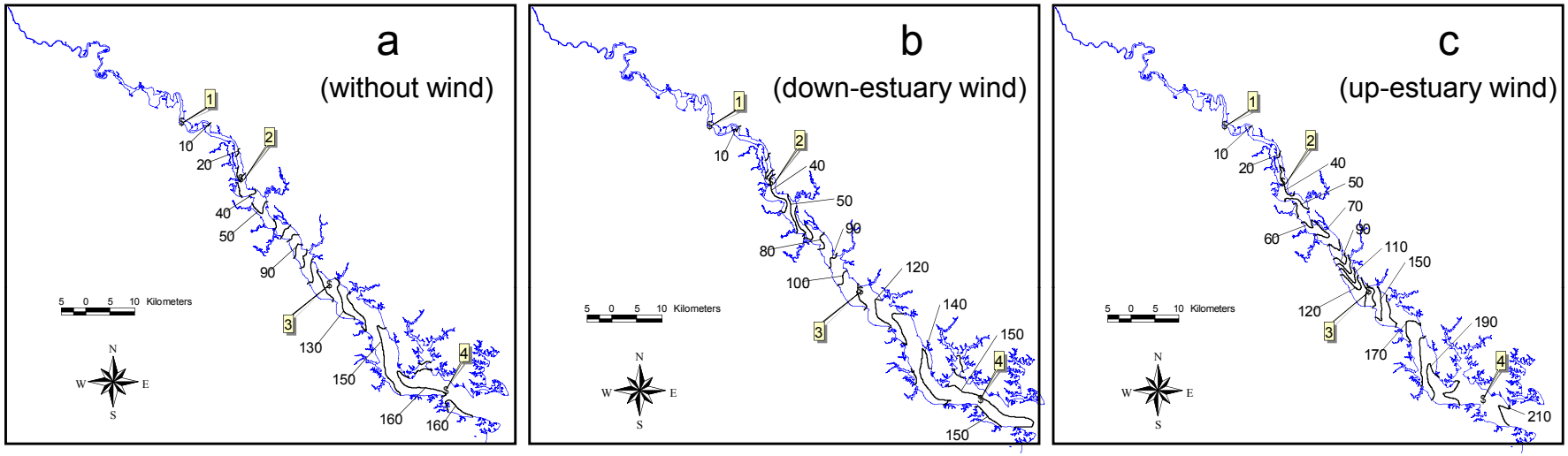

Figure 14

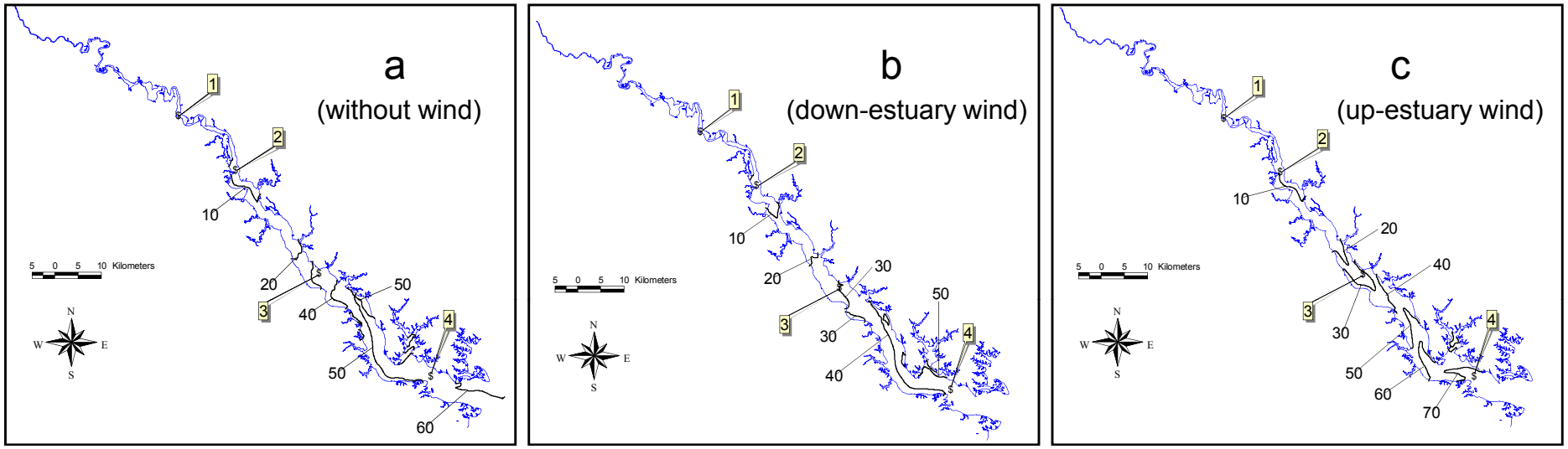

Figure 15